Efficient Short-Wave NIR Emission Induced by Energy Transfer from Cr^{3+} Clusters to Ni^{2+} in $LiAl_5O_8$: Cr^{3+}, Ni^{2+} Phosphor-in-Glass for Spectroscopy Applications

Yuqing Yan, Feifeng Huang, Guanyu Zhu, Yi Zhang, Zhexuan Gao,

Huanping Wang, Degang Deng*, Hua Yu, Shiqing Xu*

Key Laboratory of Rare Earth Optoelectronic Materials and Devices of Zhejiang Province, Institute of Optoelectronic Materials and Devices, China Jiliang University, Hangzhou 310018, People's Republic of China

Center for Advanced Optoelectronic Materials, College of Materials and Environmental Engineering, Hangzhou Dianzi University, Hangzhou 310018, China

Experiment

Materials and Synthesis

Phosphor: The $LiAl_5O_8$: $x Cr^{3+}$, yNi^{2+} phosphors with various doping concentrations were successfully synthesized by way of a hightemperature solid state. Li_2CO_3 (Aladdin, 99.99%), Al_2CO_3 (Aladdin, 99.99%), Cr_2O_3 (Aladdin, 99.95%) and NiO (Aladdin, 99.99%) were used as initial materials. The raw materials weighed on the basis of stoichiometric ratios were evenly ground in a mortar. Alumina crucibles were then used as vessels to hold the finely ground mixtures. Subsequently, they were placed in a muffle furnace sintered at 1600 °C for 2 h, and the heating rate was maintained at 7 °C/min, which contributes to a full reaction. Then samples were cooled naturally to room temperature and ground with the aim of subsequent testing.

pc-LED: The optimal $LiAl_5O_8$: $0.20Cr^{3+}$, $0.03Ni^{2+}$ phosphor was used to package the NIR pc-LED, which sufficiently mixed with glue A and glue B in conformity with the weight ratio of 1:1 on 420nm LED chip (power, 3W; voltage, 3.0-3.2V; current, 700mA; purchased from Youjing Photoelectric Original Factory), and the mixture was homogeneously stirred for 15 min and dried in an oven at 373 K for 2 h.

* Corresponding author:

E-mail address: dengdegang@cjlu.edu.cn (D. Deng). shiqingxu@cjlu.edu.cn (S. Xu).

Telephone numbers: +86-571-86835781; *Fax:* +86-571-86835781

PiG pc-LED: First of all, the prepared $LiAl_5O_8$: $0.20Cr^{3+}$, $0.03Ni^{2+}$ phosphor and commercial borate glass powders were mixed in different mass ratios and ground in a mortar for 10 min. The mixture was then pressed with a hydraulic mold at a pressure of 10 Mpa for 8 min into a disc shape. The pressed samples were then sintered in a box furnace at 450°C for 30 min. After cooling to room temperature with the furnace, the glasses were polished to fine disks with a thickness of 1.5 mm for characterizations.

Characterization

In an attempt to obtain the phase data of LiAl5O8: xCr3+ phosphors, the X-ray powder diffractometer was used with Cu Kα radiation (λ = 1.5405 Å) at 40 kV and 40 mA (Rigaku, Japan). It should be noted that the X-ray diffraction (XRD) patterns were recorded in the range of 10−80°. XRD Rietveld refinements were performed using a GSAS program. It was a field emission scanning electron microscope (SU 8010, Japan) that recorded the morphology and elemental composition data of samples. Additionally, the interplanar crystal spacing was observed by a field emission transmission electron microscope (SU 8010, America) and calculated with the help of the Gatan Microscopy Suite. PL, PLE, and Temperature-dependent NIR PL spectra of synthesized phosphors were measured by a fluorescence spectrophotometer (Edinburgh Instruments, FLSP-920) equipped with a xenon lamp as the excitation source and a temperature controller. The PL decay curves were measured with a Lecroy Wave Runner 6100 digital oscilloscope (1 GHz) using a tunable laser (pulse width = 4 ns, gate = 50 ns) as the excitation source (Continuum Sunlite OPO). The diffuse reflection (DR) spectra were monitored by UV-vis-NIR spectrophotometer (Hitachi-UH4100, Japan), taking BaSO4 powder as the base. The luminescence quantum yields of the typical phosphor was evaluated by an absolute PL quantum efficiency measurement system (Model C9920-02, Hamamatsu Photonics K.K., Japan). Electron paramagnetic resonance (EPR) spectra were recorded at RT using a Bruker spectrometer operated at 9.646 GHz (EMXplus-6/1, German). The electroluminescence PL, optical power and photoelectric conversion efficiency of NIR pc-LED devices assembled with typical phosphors were

characterized using a HAAS 2000 photoelectric measuring system (EVERFINE, China). A short-wave infrared optical camera (MV-UBS300C, MT9T001, Mind Vision, China) with an 80-ms integration time was used to acquire the NIR images.

Theoretical calculations

The lattice and electronic structures of $LiAl_5O_8$ were calculated by Vienna ab initio simulation package codes, which is based on density functional theory (DFT). The generalized gradient approximation with the Per-dew–Burke–Ernzerhof function was used for the exchange-correlation potential. In all calculations, the cut-off energy Ecut of 400 eV was used. A gamma-centered 10×10×1 k-mesh grid in the Brillouin zone was employed to determine the self-consistent charge density using the gamma-centered method. The crystal lattice was fully relaxed until the atomic force was less than 0.01 eV/Å. The energy convergence criterion for self-consistent electronic calculations was set to 10^{-4} eV/atom.

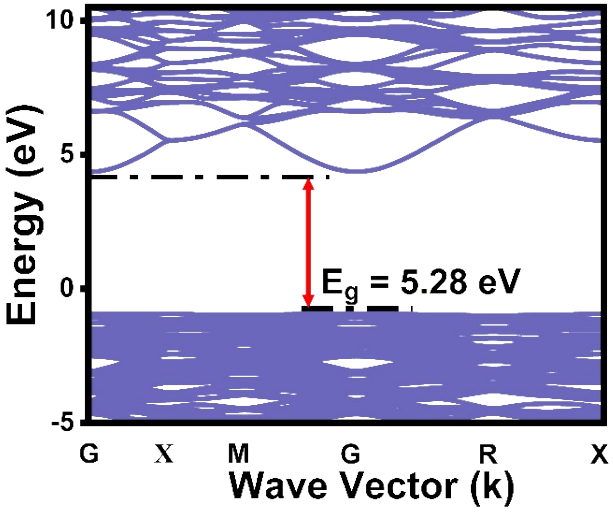

Figure S1. Band structure diagram of $LiAl_5O_8$.

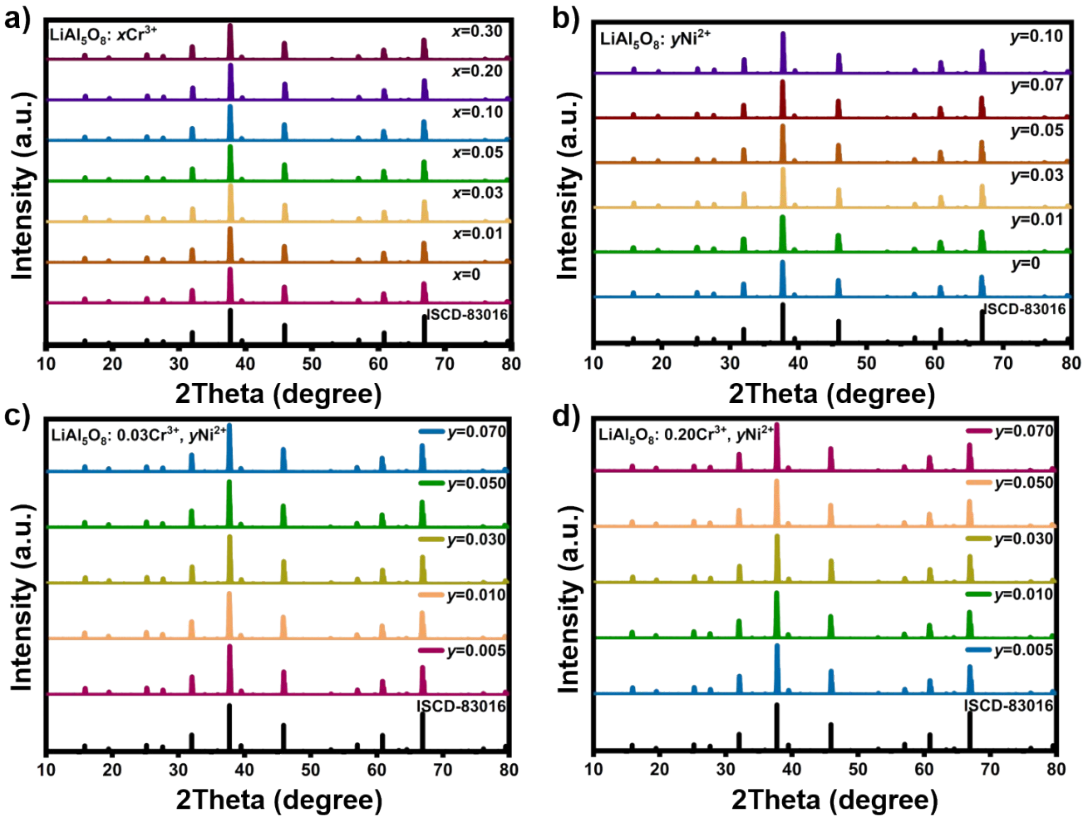

Figure S2. XRD patterns of $LiAl_5O_8$: xCr^{3+}(x=0-0.30), $LiAl_5O_8$: yNi^{2+}(y=0-0.10), and $LiAl_5O_8$: xCr^{3+}, yNi^{2+}(x=0.03/0.20, y=0-0.07) samples.

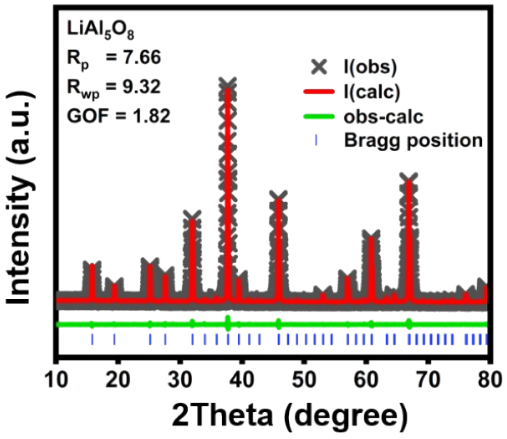

Figure S3. Rietveld refinement profiles of $LiAl_5O_8$.

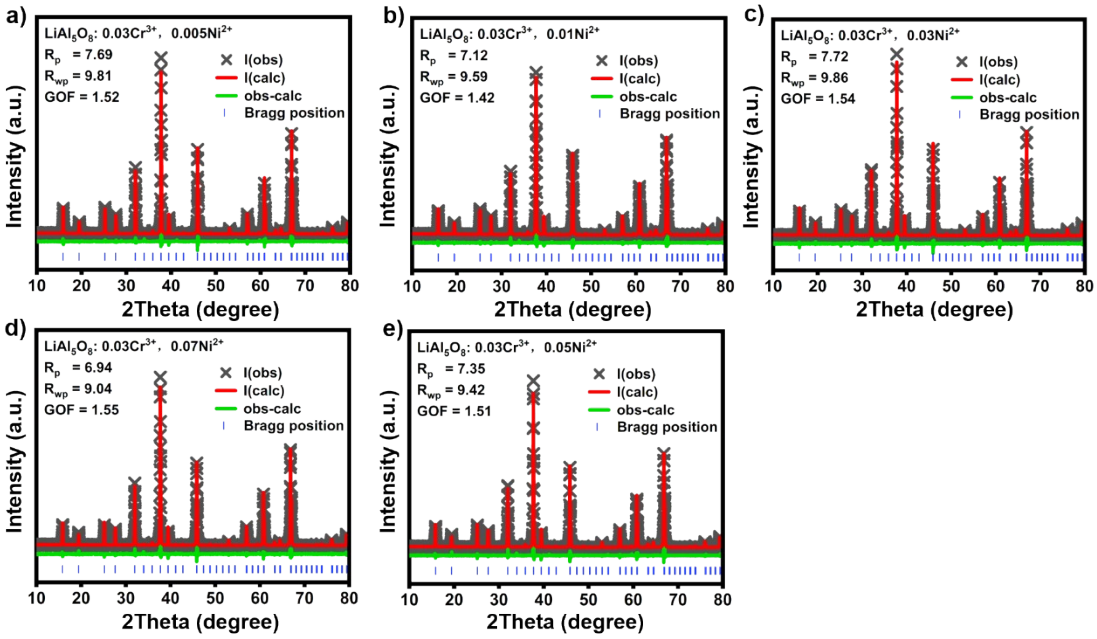

Figure S4. Rietveld refinement profiles of $LiAl_5O_8$: $0.03Cr^{3+}$, yNi^{2+}(y=0.005-0.07).

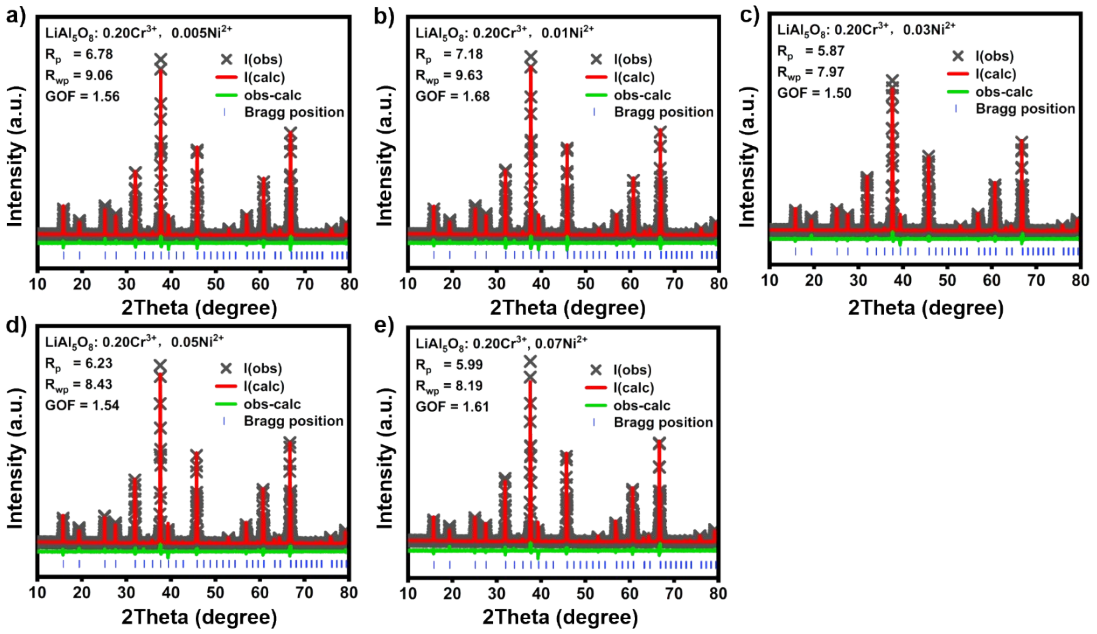

Figure S5. Rietveld refinement profiles of $LiAl_5O_8$: $0.20Cr^{3+}$, yNi^{2+}(y=0.005-0.07).

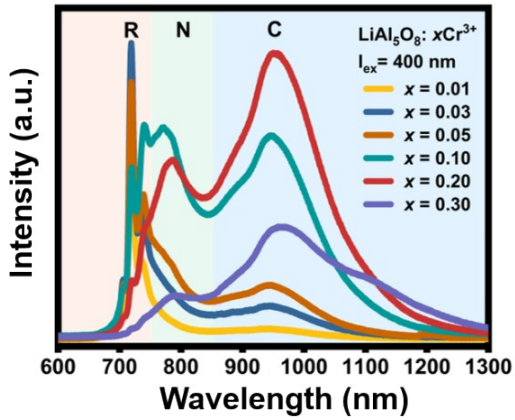

Figure S6. PL spectra of $LiAl_5O_8$: xCr^{3+} (x = 0-0.30).

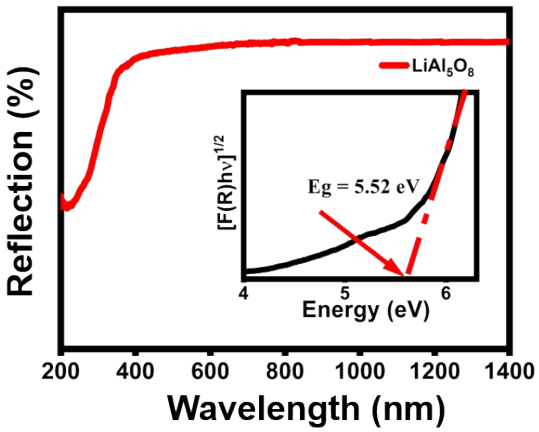

Figure S7. DRS spectra of $LiAl_5O_8$; the inset shows the relationship between $(Fhv)^{1/2}$ and hv of the $LiAl_5O_8$ host.

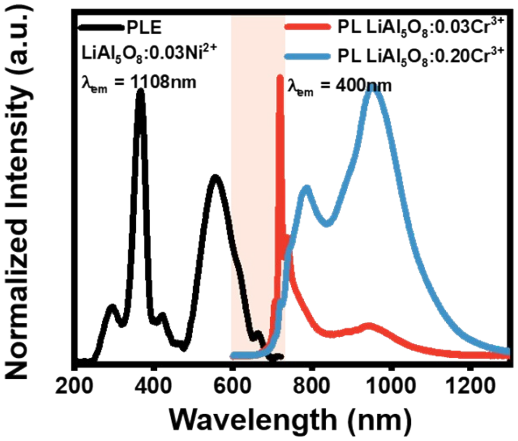

Figure S8. PL spectrum of $LiAl_5O_8$: xCr^{3+}, x=0.03 and x=0.20 upon excitation at 400nm, and the PLE spectrum of PL spectrum of $LiAl_5O_8$: 0.03Ni^{2+} monitored at1108nm.

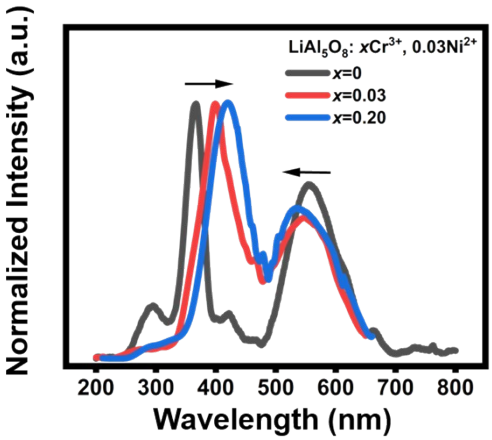

Figure S9. PLE spectra of $LiAl_5O_8$: xCr^{3+}, $0.03Ni^{2+}$(x=0,0.03,0.20).

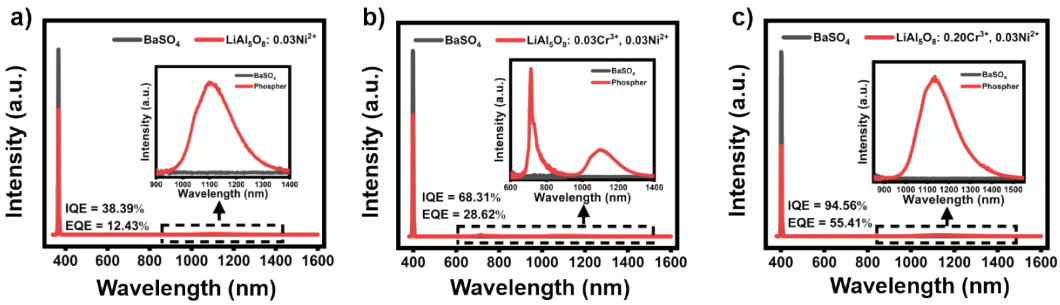

Figure S10. Emission spectra for the QY measurement of $LiAl_5O_8$: $0.03Ni^{2+}$, $LiAl_5O_8$: $0.03Cr^{3+}$, $0.03Ni^{2+}$ and $LiAl_5O_8$: $0.20Cr^{3+}$, $0.03Ni^{2+}$.

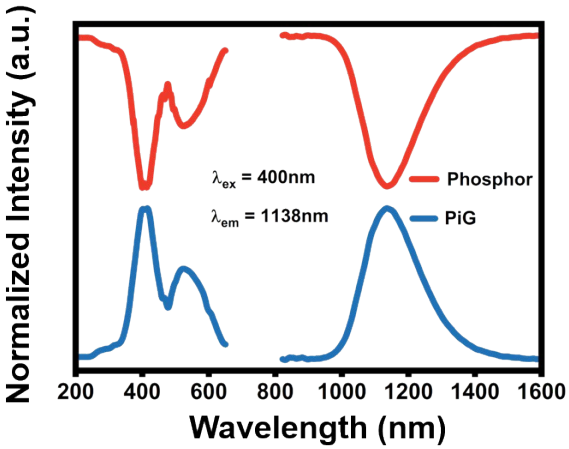

Figure S11. Photoluminescence (PL) and PL excitation (PLE) spectra of the $LiAl_5O_8$: $0.20Cr^{3+}$, $0.03Ni^{2+}$ phosphor and $LiAl_5O_8$: $0.20Cr^{3+}$, $0.03Ni^{2+}$-PiG.

Table S1. Structure parameters derived from the Rietveld refinement results of $LiAl_5O_8$: xCr^{3+} and $LiAl_5O_8$: xCr^{3+}, yNi^{2+}(x = 0.03/0.20, y = 0.005-0.070).

Cr^{3+} contents (x)	Atoms	Wyckoff position	x	y	z	Occ.	a=b=c (Å)	V (Å^3)	R_{wp} R_p χ^2
	O1	24e	0.1146	0.1329	0.3847	1			
	O2	8c	0.3859	0.3859	0.3859	1			9.32
x=0	Al1	8c	-0.0025	-0.0025	-0.0025	1			
y=0	Al2	4b	0.625	0.625	0.625	0.042	7.90971	494.859	7.66
	Li1	4b	0.625	0.625	0.625	0.957			
	Al3	12d	0.3686	-0.1186	0.125	0.986			1.82
	Li2	12d	0.3686	-0.1186	0.125	0.013			
	O1	24e	0.1146	0.1329	0.3847	1			
	O2	8c	0.3859	0.3859	0.3859	1			9.81
x=0.03	Al1	8c	-0.0025	-0.0025	-0.0025	1			
y=0.005	Al2	4b	0.625	0.625	0.625	0.042	7.91396	495.657	7.69
	Li1	4b	0.625	0.625	0.625	0.957			
	Al3	12d	0.3686	-0.1186	0.125	0.986			1.52
	Li2	12d	0.3686	-0.1186	0.125	0.013			
	O1	24e	0.1146	0.1329	0.3847	1			
	O2	8c	0.3859	0.3859	0.3859	1			9.59
x=0.03	Al1	8c	-0.0025	-0.0025	-0.0025	1			
y=0.01	Al2	4b	0.625	0.625	0.625	0.042	7.91351	495.573	7.12
	Li1	4b	0.625	0.625	0.625	0.957			
	Al3	12d	0.3686	-0.1186	0.125	0.986			1.42
	Li2	12d	0.3686	-0.1186	0.125	0.013			
	O1	24e	0.1146	0.1329	0.3847	1			
	O2	8c	0.3859	0.3859	0.3859	1			9.86
x=0.03	Al1	8c	-0.0025	-0.0025	-0.0025	1			
y=0.03	Al2	4b	0.625	0.625	0.625	0.042	7.91097	495.096	7.72
	Li1	4b	0.625	0.625	0.625	0.957			
	Al3	12d	0.3686	-0.1186	0.125	0.986			1.56
	Li2	12d	0.3686	-0.1186	0.125	0.013			
	O1	24e	0.1146	0.1329	0.3847	1			
	O2	8c	0.3859	0.3859	0.3859	1			9.42
x=0.03	Al1	8c	-0.0025	-0.0025	-0.0025	1			
y=0.05	Al2	4b	0.625	0.625	0.625	0.042	7.90973	494.863	7.35
	Li1	4b	0.625	0.625	0.625	0.957			
	Al3	12d	0.3686	-0.1186	0.125	0.986			1.51
	Li2	12d	0.3686	-0.1186	0.125	0.013			
	O1	24e	0.1146	0.1329	0.3847	1			
	O2	8c	0.3859	0.3859	0.3859	1			9.04
x=0.03	Al1	8c	-0.0025	-0.0025	-0.0025	1			
y=0.07	Al2	4b	0.625	0.625	0.625	0.042	7.90938	494.797	6.94
	Li1	4b	0.625	0.625	0.625	0.957			
	Al3	12d	0.3686	-0.1186	0.125	0.986			1.55
	Li2	12d	0.3686	-0.1186	0.125	0.013			

	O1	24e	0.1146	0.1329	0.3847	1			
	O2	8c	0.3859	0.3859	0.3859	1			9.06
x=0.20	Al1	8c	-0.0025	-0.0025	-0.0025	1			
y=0.005	Al2	4b	0.625	0.625	0.625	0.042	7.92437	497.616	6.78
	Li1	4b	0.625	0.625	0.625	0.957			
	Al3	12d	0.3686	-0.1186	0.125	0.986			1.56
	Li2	12d	0.3686	-0.1186	0.125	0.013			
	O1	24e	0.1146	0.1329	0.3847	1			
	O2	8c	0.3859	0.3859	0.3859	1			7.97
x=0.20	Al1	8c	-0.0025	-0.0025	-0.0025	1			
y=0.01	Al2	4b	0.625	0.625	0.625	0.017	7.9236	497.471	5.97
	Li1	4b	0.625	0.625	0.625	0.982			
	Al3	12d	0.3686	-0.1186	0.125	0.994			1.50
	Li2	12d	0.3686	-0.1186	0.125	0.005			
	O1	24e	0.1146	0.1329	0.3847	1			
	O2	8c	0.3859	0.3859	0.3859	1			9.63
x=0.20	Al1	8c	-0.0025	-0.0025	-0.0025	1			
y=0.03	Al2	4b	0.625	0.625	0.625	0.042	7.92181	497.134	7.18
	Li1	4b	0.625	0.625	0.625	0.957			
	Al3	12d	0.3686	-0.1186	0.125	0.986			1.68
	Li2	12d	0.3686	-0.1186	0.125	0.013			
	O1	24e	0.1146	0.1329	0.3847	1			
	O2	8c	0.3859	0.3859	0.3859	1			8.43
x=0.20	Al1	8c	-0.0025	-0.0025	-0.0025	1			
y=0.05	Al2	4b	0.625	0.625	0.625	0.042	7.90973	496.870	6.23
	Li1	4b	0.625	0.625	0.625	0.957			
	Al3	12d	0.3686	-0.1186	0.125	0.986			1.54
	Li2	12d	0.3686	-0.1186	0.125	0.013			
	O1	24e	0.1146	0.1329	0.3847	1			
	O2	8c	0.3859	0.3859	0.3859	1			8.19
x=0.20	Al1	8c	-0.0025	-0.0025	-0.0025	1			
y=0.07	Al2	4b	0.625	0.625	0.625	0.042	7.91958	496.714	5.99
	Li1	4b	0.625	0.625	0.625	0.957			
	Al3	12d	0.3686	-0.1186	0.125	0.986			1.61
	Li2	12d	0.3686	-0.1186	0.125	0.013			

Table S2. Ion Charge and Coordination Information.

Ion	Charge	Coordination	Ionic Radius
Li	+1	VI	0.76
Al	+3	VI	0.535
Cr	+3	VI	0.615
Ni	+2	VI	0.69

Theoretical calculations

The lattice and electronic structures of $LiAl_5O_8$ were calculated by Vienna ab initio simulation package codes, which is based on density functional theory (DFT). The generalized gradient approximation with the Per-dew–Burke–Ernzerhof function was used for the exchange-correlation potential. In all calculations, the cut-off energy Ecut of 400 eV was used. A gamma-centered 10×10×1 k-mesh grid in the Brillouin zone

was employed to determine the self-consistent charge density using the gamma-centered method. The crystal lattice was fully relaxed until the atomic force was less than 0.01 eV/Å. The energy convergence criterion for self-consistent electronic calculations was set to 10^{-4} eV/atom.

Kubelka-Munk function

$$F(R_\infty) = \frac{(1-R)^2}{2R}$$

$$[F(R_\infty)h\nu]^n = C(h\nu - E_g)$$

where R is the reflectance in the diffuse reflectance spectra, $h\nu$ is the photon energy, n = 2 (direct band gap) or 1/2 (indirect band gap), and C is a proportional constant.

The critical distance (R_c)

$$R_c \approx 2\left(\frac{3V}{4\pi x_c N}\right)^{\frac{1}{3}}$$

where V represents the unit cell volume, x_c represents the critical concentration (Cr^{3+}), and N is the number of cations occupied by activated ions per unit cell.

The Arrhenius formula

$$I(T) = \frac{I_0}{1 + Aexp\left(\frac{-\Delta E}{kT}\right)}$$

Where $I(T)$ is the emission intensity at temperature T, I_0 is the initial intensity, k is Boltzmann's constant (8.616×10^{-5} eV K^{-1}), and ΔE is the activation energy.

Calculation of Quantum Efficiency

$$IQE = \frac{\int L_s}{\int E_R - \int E_s}$$

$$AE = \frac{\int E_R - \int E_S}{\int E_R} \times 100\%$$

$$EQE = AE \times IQE = \frac{\int L_s}{\int E_R} \times 100\%$$

The IQE is defined as the percentage of the number of emitted photons to that of absorbed photons. where E_S stands for the spectrum of light used for exciting the

phosphor, L_S represents the emission spectrum of the phosphor, and E_R is the spectrum of excitation light without phosphor in sphere. The absorption efficiency (*AE*) is defined as the percentage of the number of absorbed photons (by the sample) to that of excitation photons. In addition, the *EQE* is defined as the percentage of the number of emitted photons to the number of exciting photons.